Accepted Manuscript

Quaternary ammonium cationic polymer as a superior bifunctional binder for lithium–sulfur batteries and effects of counter anion

Junbin Liao, Zhibin Ye

PII: S0013-4686(17)32340-X

DOI: 10.1016/j.electacta.2017.10.194

Reference: EA 30580

To appear in: *Electrochimica Acta*

Received Date: 4 May 2017

Revised Date: 16 October 2017

Accepted Date: 30 October 2017

Please cite this article as: J. Liao, Z. Ye, Quaternary ammonium cationic polymer as a superior bifunctional binder for lithium–sulfur batteries and effects of counter anion, *Electrochimica Acta* (2017), doi: 10.1016/j.electacta.2017.10.194.

Quaternary Ammonium Cationic Polymer as a Superior Bifunctional Binder for Lithium–Sulfur Batteries and Effects of Counter Anion

Junbin Liao [1] and Zhibin Ye [1,2,*]

[1] Bharti School of Engineering, Laurentian University, Sudbury, Ontario P3E 2C6, Canada

[2] Department of Chemical and Materials Engineering, Concordia University, Montreal, Quebec H3G 1M8, Canada

Correspondence to: Z. Ye (E-mail: zye@laurentian.ca or zhibin.ye@concordia.ca)

Abstract

Bifunctional polymer binders featured with both strong binding and superior polysulfide trapping properties are highly desired for the fabrication of sulfur cathodes with suppressed polysulfide shuttling in Li–S batteries. In this paper, we have explored the potential of a quaternary ammonium cationic polymer, polydiallyldimethylammonium (PDADMA-X; X = T, B, P, and Cl) with different counter anions ($TFSI^-$, BF_4^-, PF_6^-, and Cl^-, respectively) as the bifunctional binder. We have also revealed the dramatic effects of the counter anion on the performance of the cationic polymer binder. PDADMA-X's containing the former three weakly associating anions have been demonstrated to show polysulfide adsorption capability. In particular, PDADMA-T having the largest, least interacting $TFSI^-$ anion shows the

optimum performance, with strong binding strength and the best polysulfide adsorption capability. Relative to commercial PVDF and PDADMA-X's of other counter anions, it offers sulfur cathodes with lowered polarization, higher discharge capacity, significantly better capacity retention, and improved cycling stability. With its convenient synthesis from commercially available PDADMA-Cl, cationic PDADMA-T having the $TFSI^-$ anion is a promising bifunctioal binder for sulfur cathodes in practical Li-sulfur batteries.

Key words: lithium-sulfur battery, binders, cathodes, cationic polymers, counter anions.

1. Introduction

Lithium–sulfur (Li–S) batteries as a post-lithium-ion technology have recently drawn enormous research interest due to sulfur's high theoretical specific capacity (1672 mAh g^{-1}) and high energy density (2600 Wh kg^{-1}), as well as its low cost and environmental friendliness [1–6]. Despite these highly desirable features, the Li–S battery technology suffers from several technical restrictions that hinder its practical application. The dissolution of lithium polysulfides in Li–S batteries causes the long-known "polysulfide shuttling" between the electrodes, which leads to reduced Columbic efficiency, loss of active material, drastic capacity fade, high self-discharge, *etc*. The poor electrical conductivity of elemental sulfur and lithium sulfides, and volume expansion of sulfur during cycling are also the factors hindering the commercialization of Li–S batteries [1–6]. To resolve these challenges, numerous elegant strategies have been developed [1–6]. Most efforts have been focused on

designing carbon-based sulfur hosts (such as microporous/mesoporous carbons [7–14], hollow carbon nanospheres [15–18], graphenes [19–21], carbon nanotubes [22,23] and nanofibers [24,25], etc.), polar polysulfide-trapping cathode additives (such as graphene oxide [26,27], heteroatom-doped carbons [28,29], metal oxides [30,31], metal-organic frameworks [32], *etc*.), or polysulfide barriers [33–38]. These investigations demonstrate the successful suppression of "polysulfide shuttling" and the enhanced battery performance by entrapping polysulfides within the sulfur cathodes *via* physical confinement or chemical interactions.

Polymer binder is an important element in batteries by maintaining both the electronic and mechanical integrity of the battery electrodes. It is required to strongly bind the active material and conducting carbon additives together against the volume expansion to the current collector through mechanical adhesion. Though used only at small quantities (about 10 wt% of the total electrode materials), its selection affects battery performance significantly [39]. Conventional polymer binders for Li–S batteries, such as poly(vinylidenedifluoride) (PVDF), solely serve the single binding role while without the desired affinity to or trapping of the intermediate polysulfide species to ameliorate "polysulfide shuttling". Developing bifunctional cost-effective polymer binders endowed with the additional capability of trapping polysulfide species and preventing their loss from the sulfur cathodes is a new trend for Li–S batteries of improved capacity retention.

Several bifunctional polymer binders have been recently reported for Li–S batteries, showing

the valuable capability of trapping/absorbing polysulfides. These include poly(vinylpyrrolidone) (PVP) [40–43], modified natural β-cyclodextrins [44,45], natural gum Arabic [46], polyamidoamine dendrimers [47], and cross-linked polyethyleneimine [48]. As a common feature, these bifunctional binders all possess abundant polar groups (such as carboxyl, amine, imine, and hydroxyl) of strong affinity towards the polysulfide species and render Li–S batteries of significantly improved performance relative to conventional binders.

In this work, we investigate a range of quaternary ammonium-containing cationic polymers, polydiallyldimethylammonium bearing different counter anions [bis(trifluoromethane)solfonimide ($TFSI^-$), tetrafluoroborate (BF_4^-) and hexafluorophosphate (PF_6^-), choride (Cl^-); termed correspondingly as PDADMA-X, with X = T, B, P, and Cl standing for $TFSI^-$, BF_4^-, PF_6^- and Cl^- anions, respectively] as binders for Li–S batteries. These PDADMA-X polymers bearing other counter anions can be easily obtained from commercially available, cheap PDADMA-Cl having a chloride counter anion by anion exchange. Containing abundant quaternary ammonium cations (one in each repeat unit), these cationic polymers are reasoned to show strong ionic interactions with the polysulfide anions in lithium polysulfides and thus facilitate the trapping of polysulfides to render Li–S batteries of improved performance. Quaternary ammonium salts, tetrabutylammonium triflate ($NBu_4SO_3CF_3$) and N-methyl-N-butylpyrrolidinium bis(trifluoromethanesulfonyl)imide (PYR14TFSI), have been demonstrated, when introduced into the electrolyte, to stabilize the polysulfide anions through a chemical interaction with a significant improvement in the capacity retention of a Li–S cell [49]. Polymer binders bearing quaternary ammonium cations

have been previously reported to stabilize polysulfides and improve cyclic performance of Li–S batteries. Song *et al*. demonstrated that the modification of graphene oxide-sulfur composites with cetyltrimethylammonium bromide (a quaternary ammonium-containing surfactant) significantly improved battery cycling performance owing to the strong interactions between CTAB and polysulfide species [26]. Zeng *et al*. modified the β-cyclodextrin binder by introducing quaternary ammonium cations, rendering significant improvements in cyclic performance and rate capability of the cathodes [45]. In both examples, the cathode systems were quite complex due to the presence of GO or *β*-cyclodextrin that contain various polysulfide-attracting functionalities in addition to the cations. Because of the complication, the exact role of the quaternary ammonium cations has not been specified. This has intrigued us to investigate the use of PDADMA-X as the potential bifunctional binders, since they contain purely quaternary cations while with no other complicating functionalities. Their effects on the cathode performance have been systematically investigated, with a comparison made with PDADMA-Cl and conventional PVDF. Meanwhile, the effects of their counter anions on their cathode performance have also been revealed.

2. Experimental

2.1. Materials

All chemicals, including sulfur powders (100 mesh particle size, Aldrich), Super-P carbon

black (IMERYS Graphite & Carbon, Belgium), poly(vinylidene fluoride) (PVDF, Mw ~534,000 g/mol, Aldrich), bis(trifluoromethane)sulfonimide lithium salt (LiTFSI, 99.95%, Aldrich), 1-methyl-2-pyrrolidone (NMP, reagent Plus® 99%, Sigama-Aldrich), lithium nitrite ($LiNO_3$, reagent Plus®, Aldrich), poly(diallyldimethylammonium chloride) (PDADMA-Cl, high molecular weight, 20 wt.% in water, Aldrich), 1,3-dioxolane (DOL, 99%, Aldrich), 1,2-dimethoxyethane (DME, anhydrous, 99.5%, Aldrich), Super- Hydride® solution (1.0 M lithium triethylborohydride in tetrahydrofuran, Aldrich), sodium tetrafluoroborate ($NaBF_4$, 98%, Aldrich), potassium hexafluorophosphate (KPF_6, 98%, Aldrich) were used as received without further purification, except that LiTFSI was dried under vacuum for over 12 h at room temperature, and DME and DOL were dried and stored over a 4 Å molecular sieve. Other solvents, including methanol (>99%), tetrahydrofuran (THF, HPLC grade, >99%), toluene (HPLC grade), etc., were obtained from Fisher Scientific and were also dried and stored over 4 Å molecular sieves.

2.2. Preparation of PDADMA-X Bearing Different Counter Anions ($TFSI^-$, BF_4^-, and PF_6^-)

The aqueous PDADMA-Cl solution was first freeze-dried for over 120 h, rendering bulk white solid of PDADMA-Cl. The solid was further dried under vacuum at 80 ºC for 12 h. To prepare the anion exchanged PDADMA-X's, 1.0 mmol of PDADMA-Cl and 1.1 mmol of the corresponding salt (LiTFSI, $NaBF_4$, KPF_6, respectively) bearing the desired counter anion were separately dissolved in 40 mL methanol. Subsequently, the as-prepared PDADMA-Cl solution in methanol was added drop by drop into the salt solution under rapid agitation,

rendering the immediate precipitation of the anion-exchanged polymer. The white polymer suspension was subsequently centrifuged and the resultant anion-exchanged polymer was washed with an excessive amount of methanol three times, followed by drying under vacuum at 80 ºC for 12 h.

2.3. Polysulfide Adsorption Test

A lithium polysulfide standard Li_2S_4 was prepared by modifying a literature procedure [30]. In an argon-filled glove box, sulfur was dissolved in Super-Hydride® solution (1.0 M lithium triethylborohydride in THF), with a Li to S mole ratio of 1:2. The resulting solution was dried under vacuum, followed by a final wash with hexane and centrifugation to isolate the yellow precipitate, Li_2S_4 (see the insert in **Fig. 2(a)**).

Adsorption of Li_2S_4 with the five different binders was undertaken at two different binder/Li_2S_4 mass ratios of 12.5:1 and 1:1. Typically, the binder at a known mass was added into a known volume of Li_2S_4 solution (concentration, 0.4 mg mL^{-1}) in mixed DME-DOL solvent (volume ratio, 1:1). The supernatant solution was monitored with UV-vis spectroscopy (Varian Cary 100). Typically, 40 mg of each binder was added into 8 mL of Li_2S_4 solution in DME-DOL; containing 3.2 mg Li_2S_4), where the mass ratio of the binder to $Li2S_4$ is 12.5:1. UV-vis measurement was carried out on the supernatant solution after a prescribed time to monitor the adsorption.

To obtain spectroscopic evidence confirming the adsorption of Li_2S_4, x-ray photoelectron spectroscopy (XPS) measurements of PDADMA-T containing the adsorbed Li_2S_4, pure PDADMA-T and pure Li_2S_4 were undertaken on a Thermo Scientific Theta Probe XPS spectrometer (Thermo Fisher). A monochromatic Al Kα X-ray source was used, with a spot area 400 μm. The samples were run in a standard mode, i.e., all angle collected (60° angular acceptance) for the survey spectra, and for the region spectra.

2.4. Electrode Fabrication

The sulfur/carbon composite was prepared by grinding elemental sulfur and super-P at a mass ratio of 3:1 in a mortar, and followed with melt infusion at 155 ºC for 12 h in a sealed glass tube. The sulfur content in the resulting composite is 74.7 wt% as per thermogravimetric analysis (TA Instruments Q50 TGA at a heating rate of 10 ºC min^{-1}). The slurries for sulfur electrodes were prepared by adding a known mass (400 mg) of S/C composite into the solution containing the prescribed mass of the binder (PDADMA-X or PVDF; 50 mg) and super-P carbon black (50 mg) in NMP (for all binders except PDADMA-Cl; 3 mL) or methanol (for PDADMA-Cl; 3 mL) to achieve a final S/C/binder ratio of 60:30:10, followed with thorough mixing with a mechanical stirrer. Electrodes were prepared by evenly depositing a known volume (16 or 48 μL) of each slurry on carbon-coated aluminum foil (0.018 mm in thickness, 1.32 cm^2 in area) as the current collector. The sulfur loading for all electrodes was all controlled at *ca.* 1.0 or 3.0 mg cm^{-2}. The electrodes were dried in an oven at 65 ºC for 5 h, then in a vacuum oven at 50 ºC prior to use.

2.5. Electrochemical Testing

Electrochemical performances of the sulfur electrodes prepared with the different binders were tested in CR2032-type coin cells. All the cells were assembled in an Ar-filled glove box. The electrolyte employed contained 1.0 M LiTFSI in a binary solvent of DOL and DME (1:1 in volume) with 2 wt% $LiNO_3$ as additive. An electrolyte volume of *ca.* 20 μL or 35 μL was employed for electrodes with sulfur loading of 1.0 and 3.0 mg cm^{-2}, respectively. Lithium metal foil was used as the negative electrode, and was physically separated from the sulfur cathode with two sheets of Celgard 2500 separators. The cells were tested through galvanostatic charge/discharge (GCD) cycling at room temperature on a LAND CT2001A battery testing system. Current density and specific capacity were calculated based on the mass of sulfur active material.

Cyclic voltammetry (CV) measurements of the cells were all recorded on a Metrohm Autolab PGSTAT128N electrochemical work station in the voltage range of 1.5–3.0 V *vs*. Li^+/Li at a scan rate of 0.1 mV s^{-1}. Electrochemical impedance spectroscopy (EIS, Metrohm Autolab PGSTAT128) measurement was carried out from 10 mHz to 100 kHz at room temperature with a potentiostatic signal amplitude of 5 mV.

3. Results and discussion

3.1 Polysulfide Adsorption with PDADMA-X

A PDADMA-Cl-resembling cationic copolymer polyelectrolyte bearing the same quaternary ammonium ion with chloride counter ion, poly(acrylamide-co-diallyldimethylammonium chloride) (AMAC), has been previously used by Zhang as the binder for Li-S batteries [50]. Due to its nonsolubility in organic solvents, AMAC was reported to form the stable void structure in the sulfur cathode during battery cycling, rendering significantly higher capacity and better-maintained capacity retention compared to the cathodes fabricated with poly(ethylene oxide) as the binder. But AMAC having the chloride counter ion causes severe corrosion of the aluminum current collector. No polysulfide trapping capability was demonstrated with AMAC therein, despite our reasoning of possible ionic interactions between its quaternary ammonium cations and the polysulfide anions in lithium polysulfide species. This should result from too strong ionic interactions between the cation and the chloride counter ion, which prevents the anion exchange with polysulfide for trapping. We hypothesize that replacing the chloride anion in PDADMA-Cl with weakly interacting counter anions (such as $TFSI^-$, BF_4^-, and PF_6^- [51]) should facilitate the possible adsorption/trapping of polysulfide species by anion exchange (see **Figure 1(b)**), which will subsequently help suppress polysulfide shuttling and improve battery capacity retention. We have thus prepared the range of PDADMA-X (X = $TFSI^-$, BF_4^-, and PF_6^-) polymers bearing the different counter anions from PDADMA-Cl by simple convenient anion exchange. The repeat unit structures of the polymers are presented in **Figure 1(a)**.

(Figure 1)

To verify our hypothesis, we have first studied the interactions between a polysulfide standard, Li_2S_4, and the various PDADMA-X polymers, by investigating polysulfide adsorption on the polymers. To a Li_2S_4 solution in DOL/DME was added each individual polymer, with the same polymer/Li_2S_4 mass ratio of 12.5:1. Parallel experiments were also undertaken with PVDF and PDADMA-Cl, respectively, for the purpose of comparison. **Figure 2(a)** shows the color changes of the Li_2S_4 solutions after exposure to the various polymers for 5 min and 24 h, respectively, relative to the grass green blank Li_2S_4 solution. The colors of the two solutions exposed to PDADMA-T and PDADMA-P are quickly lightened within just 5 min, indicating the fast adsorption of the polysulfide species with these two polymers. On the contrary, no obvious color changes are observed for the other solutions after 5 min. After 20 h, the two solutions exposed to PDADMA-T and PDADMA-P have become completely colorless, and the one exposed to PDADMA-B also has a significantly lightened color. Meanwhile, the originally white colored polymer solids in these solutions have turned brown. These phenomena confirm the effective adsorption of the polysulfide species with the three polymers containing weakly interacting counter anions. However, negligible color changes can be seen with the other solutions exposed to PDADMA-Cl and PVDF, respectively, confirming that they do not have the affinity toward polysulfides. The ability of the three PDADMA-X polymers in adsorbing Li_2S_4 is further demonstrated with *ex situ* UV-vis spectroscopy. **Figure 2(c)** compares the UV-vis spectra of the various solutions after exposure for 24 h. While no change is observed in the spectra of

solutions exposed to PDADMA-Cl and PVDF relative to the blank solution, much lowered absorbance spectra (within 270–500 nm) are found with the solutions exposed to the other three polymers. In particular, according to the reductions of the UV-vis spectra, we can reason that the polysulfide-adsorbing capability of the three polymers increases in the order, PDADMA-Cl (PVDF) << PDADMA-B < PDADMA-P < PDADMA-T. This agrees well with the increasing radii of Cl^- (2.70 Å), BF_4^- (3.44 Å), PF_6^- (3.60 Å), and $TFSI^-$ (4.39 Å) following the order [52], confirming that increasing anion size reduces the cation-anion interactions and subsequently improves the polysulfide adsorption capability of the cationic polymers. Having too strong cation-anion interaction, PDADMA-Cl is completely ineffective for the adsorption of polysulfide species as confirmed herein.

(Figure 2)

We have also investigated the polysulfide adsorption at a reduced polymer loading (polymer/Li_2S_4 mass ratio of 1:1). **Figure 2(b)** shows the solutions after exposure to different polymers for 2 h; Figure 2(d) compares their UV-vis spectra. While the color changes of the solutions are not as clear as in **Figure 2(a)**, the three polymer solids (PDADMA-B, PDADMA-P, PDADMA-T) have become brown-colored, confirming their adsorption of the polysulfide. This is also confirmed from the appreciably lowered UV-vis spectra (within 350–500 nm) of the solutions relative to the blank solution (see **Figure 2(d)**), despite the significantly reduced polymer loading. Meanwhile, the same order of polysulfide adsorption capability of the polymers can be found from **Figure 2(d)**. These adsorption experiments thus

offer the solid evidence confirming the capability of PDADMA-X in adsorbing polysulfide with PDADMA-T being the best one. PDADMA-X's (X = B, P, and T) have thus been subsequently investigated as the binder for the Li–S batteries.

To obtain spectroscopic evidence confirming the interaction between lithium polysulfide and PDADMA-T, XPS characterization of PDADMA-T containing the adsorbed Li_2S_4 was undertaken, along with pure PDADMA-T and Li_2S_4 for comparison. Figure 3 compares their XPS spectra. A broad peak with multiple deconvoluted constituting peaks in the range of 160–165 eV is seen in the S_{2p} spectrum of Li_2S_4 (Figure 3(a)), arising from its polysulfide anion. In particular, the constituting peaks centered at 161.1 eV and 163.4 eV in S_{2p} spectra) can be ascribed to the terminal (S_T^{-1}) and bridging sulfur (S_B^0) atoms of Li-S-S-S-S-Li, respectively, where the sulfur atoms at both ends have a formal charge of (-1) while those in the middle bear a formal charge of (0), as previously shown by Nazar *et al*. and Yoon *et al*. [53,54]. PDADMA-T with adsorbed Li_2S_4 also shows the broad polysulfide peak (**Figure 3(b)**), while it is absent in the spectrum of pure PDADMA-T (**Figure 3(c)**). In addition, a small shift of $\Delta E = 0.2$ eV to a lower binding energy is observed after the capture of Li_2S_4 by PDADMA-T, which can be attributed to the electropositive nature of tetralkyl ammonium ions on PDADMA-T, which forces electrons away from the terminal sulfur [55,56], resulting in a slight decrease in the binding energy. Correspondingly, the binding energy of lithium atom in Li_2S_4 in **Figure 3(d–f)** increases from 55.1 eV to 55.4 eV upon adsorption, possibly, due to the strengthened interaction resulting from the increased polarity of polysulfide. Owing to the electropositive nature, the binding energy of nitrogen atom in PDADMA-T also

shifts to higher values (from 401.1 eV to 402.5 eV; from 397.9 eV to 399.4 eV, see **Figure 3(g–i)**) after the adsorption of Li_2S_4. The XPS evidence thus confirms the adsorption of lithium polysulfide on PDADMA-T and their interactions.

(Figure 3)

3.2 Evaluation of Binding Strength

As a binder, binding strength is an important parameter to a binder [39,45]. The binding strengths of PDADMA-X have been evaluated, with a comparison made to PVDF. Electrodes were prepared from a melt-infused sulfur/Super P composite with different polymers as the binder (sulfur: Super P: binder = 60:30:10 in mass ratio for all cathodes in this study). **Figure 4(a)** shows the images of representative fresh-made electrodes. All electrodes show visually smooth rather uniform surface, except the one made with PDADMA-Cl that shows rough non-uniform surface with the presence of light-colored domains having higher PDADMA-Cl content. Meanwhile, pitting corrosion of the aluminum current collector was observed in all the electrodes made with PDADMA-Cl due to its corrosive chloride ion, as reported by Zhang, when using the similar cationic copolymer polyelectrolyte AMAC [50]. On the contrary, no corrosion of the aluminum current collector was seen when PVDF or the anion-exchanged PDADMA-X's was used.

(Figure 4)

The different electrodes were soaked in the electrolyte solution (1 M LiTFSI in mixed DME/DOL solution) in a sealed vial for 2 weeks. After one week of soaking at room temperature, the electrolyte solution was heated to 95 ºC and kept for 30 min, then maintained at room temperature for another week. The binding strength is evaluated by comparing the amount of visible black particles that peel off from the electrodes [57]. **Figure 4(b)** shows the resulting electrolyte solutions used for soaking the different electrodes. One can see that fine suspended black particles are present in almost all solutions. However, the solutions for soaking electrodes fabricated with PDADMA-Cl and PDADMA-P contain obviously much more fine particles than the other solutions. This indicates that PVDF, PDADMA-T, and PDADMA-B have better binding performance than PDADMA-Cl and PDADMA-P. In the case with PDADMA-Cl, the relatively poorer binding performance may result from the non-uniform distribution of the composite materials on the electrodes. On the contrary, with PDADMA-P, the result suggests its relatively weaker binding strength to retain the mechanical integrity of the electrodes.

3.3 Cyclic Voltammetry (CV) Tests

CV (voltage range: 1.5–3.0 V at 0.1 mV s^{-1}) tests were undertaken on the cathodes fabricated with the five different polymers (sulfur loading density: 1.0 mg cm^{-2}). **Figure 5(a)–(e)** shows the first 10 cycles of CV curves of the cathodes. All CV curves consist of one oxidation peak and two reduction peaks characteristic of the sulfur cathodes. No additional peaks are found,

indicating that all the polymer binders are stable within the voltage range and do not participate in the reduction/oxidation process of sulfur [45]. For all cathodes, the positions of reduction peaks in the 1st cycle deviate significantly from those of the following 9 scans, which indicate the activation of cathodes during the 1st cycle. From the 2nd scan, the peak positions of all cathodes except that with PDADMA-P appear stable, with the oxidation peak at 2.5 V and two reduction peaks centered at 2.3 and 2.0 V, respectively. While the first reduction peak at 2.3 V represents the reduction of elemental sulfur to soluble high-order Li_2S_x ($4 \leq x \leq 8$), the second reduction peak at 2.0 V corresponds to their further reduction to lower order polysulfide Li_2S_x ($x < 4$) and finally to Li_2S. In the anodic scans, the oxidation peak is attributed to the gradual conversion of Li_2S back to elemental sulfur.

The cathode fabricated with PDADMA-P shows a slight but distinct left shift (2.30 to 2.27 V and 2.00 to 1.98 V, respectively) of both reduction peaks from the 2nd to 10th cycle, along with a concomitant broadening and slight right shift of the oxidation peak (from 2.51 to 2.55 V) (see **Figure 5(d)**). This indicates the gradual increase of polarization upon the dynamic volume change during cycling. A similar, but much weaker trend is also noticed with the cathode fabricated with PDADMA-Cl (see **Figure 5(b)**). The slight increased polarization is also indicative of the inferior binding performance of PDADMA-P and PDADMA-Cl as shown above, which leads to a gradual deterioration in the electrical contact within the cathode upon dynamic volume change during cycling. On the contrary, the well-retained peak positions with the other cathodes (with PDADMA-T, PDADMA-B, and PVDF) suggest the better binding performance of the other polymers against the volume change.

(Figure 5)

Distinct differences in the capacity stability among the cathodes can also be noted from their CV curves. The cathode fabricated with PVDF shows significant decreases in the current for all the redox peaks (more obviously seen with the reduction peak at 2.0 V and the oxidation peak due to their higher intensities) from 2^{nd} to 10^{th} cycle (see **Figure 5(a)**), indicating the significant capacity decay with PVDF due to polysulfide loss. The one fabricated with PDADMA-Cl instead shows a current decrease in the reduction peak at 2.3 V and simultaneously a significant current increase in the other reduction peak at 2.0 V from the 2^{nd} to 10^{th} cycle. While the former decrease indicates the gradual loss of soluble polysulfides from the cathode due to the incapability of PDADMA-Cl for their capturing, the latter increase possibly indicates the rather poor distribution of insoluble Li_2S_2 and Li_2S due to the non-uniform distribution of the carbon-sulfur composites on the electrode. These may contribute to the low sulfur utilization in the cathode with PDADMA-Cl.

On the contrary, those fabricated with PDADMA-T and PDADMA-B, respectively, show much more stable CV curves, with only minor changes in the current for all the peaks over cycling (**Figure 5(c)** and **(d)**). Though showing slight peak shifts illustrated above, the two reduction peaks of the cathode fabricated with PDADMA-P also have relatively stable current upon cycling. These confirm the improved capacity retention with the use of PDADMA-T, PDADMA-B, and PDADMA-P having the capability for polysulfide

adsorption, which helps suppress polysulfide shuttling. In particular, among all cathodes, the one fabricated with PDADMA-T shows the best-retained capacity with negligible changes in the current for all redox peaks, confirming the reversible charge-discharge process. This is in good agreement with its best polysulfide adsorption capability demonstrated above.

In addition, **Figure 5(f)** compares the 10^{th} cycle CV curves of the various cathodes. The cathodes made with PDADMA-T and PDADMA-B show much sharper and narrower oxidation peak compared to the others. Meanwhile, the one made with PDADMA-T also shows the narrowest reduction peaks, with the smallest polarization of 0.46 V observed among all the cathodes. These results suggest better, more homogeneous dispersion of finer sulfur composite particulates for redox reactions with PDADMA-T, besides its polysulfide trapping capability.

3.4 Galvanostatic Charge-Discharge Tests

Galvanostatic charge-discharge tests within a voltage range of 1.5–3.0 V were undertaken on the various cathodes having a sulfur density of 1.0 mg cm^{-2}. **Figure 6** shows the rate performance of the various cathodes tested at increasing currents ranging from 0.2C to 3C (1C = 1672 mA g^{-1}) with 10 cycles at each current, followed with 10 cycles back at 0.2 C. For all cathodes, a consistent capacity reduction is observed with the gradual current increase from 0.2C to 3C, along with the capacity recovery upon the switch of the current back to 0.2C. Among all cathodes, the one made with PDADMA-Cl shows the lowest capacity at all

currents (e.g., reversible capacity of only *ca*. 550 mA h g^{-1} at 0.2C relative to the values of 815–860 mA h g^{-1} found with the others) though with reasonable capacity retention upon the current increase. This suggests the poorest sulfur utilization in the case with PDADMA-Cl. It is reasoned to result from non-uniform distribution of larger sulfur composite particulates across the electrode as seen from **Figure 4(a)**, leading to deteriorated electrical contact between the sulfur active material and the current collector. Meanwhile, the pitting corrosion of the current collector by PDADMA-Cl is also reasoned to deteriorate the electric contact within the cathode. For the cathodes made with PDADMA-T, PDADMA-B, and PVDF, similar capacity and capacity retention with no distinctive differences are observed, with the typical reversible capacity values of 840, 740, 650, 490, and 360 mA h g^{-1} at 0.2C, 0.5C, 1C, 2C, and 3C, respectively. However, the cathode made with PDADMA-P shows relatively poorer rate performances compared to others. While it has similar capacity values as others at relatively low currents (0.2C, 0.5C, and 1C), its capacity values at enhanced currents (455 and 300 mA h g^{-1} at 2C and 3C, respectively) are appreciably lower compared to the corresponding values of others. This suggests the deteriorated electric contact and increased resistance within the cathode made with PDADMA-P at high currents, which is consistent with its relatively poorer binding strength seen above.

(Figure 6)

Figure 7(a) compares the cycling performances of the cathodes (sulfur loading density: 1.0 mg cm^{-2}) within 1.5–3.0 V for 65 cycles at 0.2C. This voltage window for cycling is much

broader than those typically used (e.g., 1.7–2.8 V or even narrower) for sulfur cathodes. It is intentionally chosen herein to evaluate the cycling performances under more severe conditions involving more thorough redox reactions. **Figure 7(b)** compares their 50^{th} cycle charge-discharge voltage profiles. Consistent with the redox peaks seen in their CV curves, all cathodes show the typical two-plateau discharge curves with a short upper plateau at 2.3 V and a long lower plateau at ca. 2.1 V, as well as a long charge plateau. For all cathodes, the branches of discharge curves below 1.8 V appear to be relatively noisy, which should result from the formation of excessive insulating Li_2S_2/Li_2S at too low discharge voltage and thus deteriorated electrical contact. Among the various cathodes, we note from **Figure 7(b)** that the cathode fabricated with PDADMA-T shows the smallest polarization (Δ V = 0.16 V) with the lowest charge plateau and the highest second discharge plateau. This trend is observed throughout the whole cycling process, indicating the improved electron transfer kinetics for the sulfur species with PDADMA-T as the binder [58]. The cathode with PDADMA-P shows the highest polarization of 0.20 V while the other with PDADMA-B, PVDF and PDADMA-Cl have the intermediate polarizations. In consistency with the results demonstrated above, this also suggests the better binding performance of PDADMA-T than PVDF.

From **Figure 7(a)**, the cathodes fabricated with PDADMA-T and PDADMA-P show similar initial capacity values (899 and 914 mA h g^{-1}, respectively), while those made with the other polymers have relatively lower initial capacities (825, 779, and 720 mA h g^{-1} with PDADMA-B, PVDF, and PDADMA-Cl, respectively). Gradual decay of the discharge

capacity can be seen with all the cathodes over 65 cycles, indicating the occurrence of polysulfide shuttling. The exception is that with PDADMA-Cl, which undergoes a rapid capacity drop to 562 mA h g^{-1} at the 3rd cycle and remains relatively stable at *ca.* 580 mA h g^{-1} afterwards over the rest 62 cycles. The cathode with PVDF shows a small capacity increase (to 851 mA h g^{-1}) within the first 5 cycles followed with the pronounced decrease afterwards. Herein, the initial capacity increase suggests the gradual cathode activation through slow electrolyte diffusion.

Though having similar initial capacities, the cathodes show different capacity retentions after 65 cycles, with the remaining capacity values of 667, 618, 600, 575 mA h g^{-1} with PDADMA-T, PDADMA-B, PDADMA-P, and PVDF, respectively, which correspond to capacity decays of 0.39, 0.39, 0.53, 0.54% per cycle, respectively, relative to the maximum/initial capacity values of each cathode. Meanwhile, for both cathodes fabricated with PDADMA-P and PVDF, the most severe capacity decrease occurs within cycles 25–40, followed with a rather flattened capacity plateau afterwards (see **Figure 7(a)**). This phenomenon is indicative of severe shuttling occurring within the period. On the contrary, the capacity decay for the cathodes with PDADMA-T and PDADMA-B are rather steady over the whole cycling process, with a linear capacity decrease over cycling. In particular, PDADMA-T offers higher capacity and significantly improved capacity retention than PVDF over the whole cycling process. Though not avoiding polysulfide shuttling, both PDADMA-T and PDADMA-B can thus suppress the shuttling at the current due to their capability of adsorbing polysulfide species as shown above besides their better binding performance. On

the contrary, due to its poorer binding strength, PDADMA-P does not improve the cycling performance despite its capability for polysulfide adsorption.

We have further undertaken cycling of the various cathodes within 1.5–3.0 V at 0.5C. **Figure 7(c)** compares their discharge capacity curves. At this enhanced current, we have found that the cathodes fabricated with PVDF, PDADMA-B, and PDADMA-P became unstable and display continuous charging at the 49^{th}, 88^{th}, and 102^{nd} cycle, respectively, along with the severe drop of Columbic efficiency to nearly zero. This phenomenon is indicative of the severe loss of sulfur active material from the cathodes. On the contrary, the cathode with PDADMA-T was stable for the entire 200 cycles though with a gradual capacity decay from *ca.* 620 to 435 mA h g^{-1} (i.e., 0.15% per cycle) and the gradual decrease of Columbic efficiency from 100% at the first cycle to 96% at the 200^{th} cycle. This comparison further confirms the best efficiency of PDADMA-T in suppressing polysulfide shuttling among the binders and in maintaining cycling performance of the cathodes.

(Figure 7)

To realize the practical application of Li-S batteries, a high sulfur loading is necessary [47]. Herein, cathodes at higher sulfur loading (3.0 mg cm^{-2}) were also fabricated with PDADMA-T and PVDF, respectively, and were tested for their cycling performance. **Figure 8** compares their discharge capacity of the cathodes within a voltage window of 1.7–2.8 V over 200 cycles, with the first cycle at 0.05C and all the rest at 0.2C. The cathode with

PDADMA-T displays a much higher initial discharge capacity (901 *vs*. 273 mAh g^{-1} at 0.05C) than that with PVDF. Subsequently, the discharge capacity of the former gradually decreases from 574 mAh g^{-1} at the 4^{th} cycle to 424 mAh g^{-1} at the 200^{th} cycle. On the contrary, the discharge capacity of the latter is generally much lower throughout and shows a slight increase from 190 mAh g^{-1} at the 2^{nd} cycle to 236 mAh g^{-1} at the 200^{th} cycle. In addition, the cathode with PDADMA-T also shows superior areal capacity, outperforming that with PVDF over the whole cycling process. For example, the cathode with PDADMA-T show a much higher discharge areal capacity (4.86 mAh cm^{-2} at 0.05C at the 1^{st} cycle; 2.56 mAh cm^{-2}at the 200^{th} cycle) relative to that with PVDF (1.31 mAh cm^{-2} at the 1^{st} cycle; 1.22 at the 200^{th} cycle). These results suggest that, at the high sulfur loading, PDADMA-T, with its ionic nature, is even more beneficial than PVDF by improving the transfer of Li^{+} within the cathodes besides its polysulfide adsorption capability.

(Figure 8)

3.5 EIS Tests

To gain further understanding of the electrochemical performance, EIS tests were undertaken on the various cathodes (sulfur loading density: 1.0 mg cm^{-2}) before any testing and after the 16^{th} cycle of charge-discharge (between 1.7–2.8 V at 0.2C). **Figure 9(a)** and **(b)** compares the Nyquist plots of the fresh cathodes before cycling and the cathodes after cycling, respectively. From **Figure 9(a)**, all fresh cathodes show a depressed semicycle assigned to charge transfer

resistance in the high-frequency region and an inclined line corresponding to Warburg impedance at the low-frequency region. One notable difference is seen with the cathode fabricated with PDADMA-P, which has a much greater charge transfer resistance (*ca.* 500 Ω vs. 180–300 Ω) than the other cathodes. In consistency with above results, this is also suggestive of the inferior electric contact within the cathode with PDADMA-P.

After cycling, all cathodes except that with PDADMA-P shows two distinct semicycles (see the insert), with overall charge transfer resistance significantly reduced compared to those of the fresh cathodes due to their activation (including the electrolyte wetting of composite and the formation of conductive soluble Li_2S_x ($4 \leq x \leq 8$) from insulated solid sulfur) after cycling (see **Figure 9(b)**) [59,60]. In particular, the semicycle in the high frequency range reflecting the charge transfer at the conductive agent surface and the other one in the medium frequency range attributable to the formation of nonconductive Li_2S/Li_2S_2 [61,62]. Among the cathodes, the former semicycle is the smallest with the cathode fabricated with PDADMA-T, confirming the best electric contact, while its second semicycle is the largest, indicating the best polysulfide adsorption capability with PDADMA-T [62]. In the case of the cathode with PDADMA-P after cycling, its charge transfer resistance still remains the largest among the cathodes, with no distinct semicycle found attributable to the formation of Li_2S/Li_2S_2.

(Figure 9)

All above results suggest that PDADMA-T shows superior performance as a bifunctional

binder for sulfur cathodes, outperforming other PDADMA-X polymers bearing different counter anions as well as commercial PVDF. These results also demonstrate the dramatic effects of the counter anions on the performance of this group of cationic polymers as binders. Herein, $TFSI^-$ having the largest anion size renders PDADMA-T as a bifunctional binder with the best polysulfide adsorbing capability. Meanwhile, with its bulky organic anion structure, it also improves the affinity of the cationic polymer toward the carbon-sulfur composites. This contributes to the improved dispersion of the composites for enhanced sulfur utilization and the enhanced binding strength for maintaining the mechanical and electrical integrity of the cathodes against drastic volume change during cycling.

4. Conclusions

We have systematically investigated in this paper the performance of quaternary ammonium cationic polymers PDADMA-X (X = T, P, B, and Cl) bearing different counter anions ($TFSI^-$, PF_6^-, BF_4^-, and Cl^-, respectively) as binders for sulfur cathodes in Li–S batteries. The former three bearing weakly interacting anions have been demonstrated to adsorb/trap lithium polysulfide species, with the trapping capability increase in the order of PDADMA-B < PDADMA-P < PDADMA-T. On the contrary, like PVDF, PDADMA-Cl bearing strongly interacting Cl^- is completely ineffective of polysulfide trapping. Electrochemical tests confirm that PDADMA-T bearing the optimum $TFSI^-$ anion shows superior performance as a bifunctional binder, with the resulting cathodes displaying the lowest capacity decay, lowest polarization, and best maintained cycling stability relative to cathodes fabricated with PVDF

and others PDADMA-X polymers. Changing the anion to PF_6^-, BF_4^-, or Cl^- leads to various deteriorations in their binding performance. This is the first demonstration of the dramatic effects of the counter anions on the binding performance of these cationic polymers.

Acknowledgements

We thank the funding support from the Canada Research Chair (CRC, Grant #230723) and the Natural Science and Engineering Research Council (NSERC) of Canada (Grant # (#477901-2015).

References

[1] A. Manthiram, S. Chung, C. Zu, Lithium−sulfur batteries: progress and prospects, Adv. Mater. 27 (2015) 1980–2006.

[2] Z. Seh, Y. Sun, Q. Zhang, Y. Cui, Designing high-energy lithium−sulfur batteries, Chem. Soc. Rev. 45 (2016) 5605–5634.

[3] Q. Pang, X. Liang, C. Kwok, L. Nazar, Advances in lithium−sulfur batteries based on multifunctional cathodes and electrolytes, Nature Energy 1 (2016) 16132.

[4] S. Urbonaite, T. Poux, P. Novák, Progress towards commercially viable Li−S battery cells, Adv. Energy Mater. 5 (2015) 1500118.

[5] Z. Li, Y. Huang, L. Yuan, Z. Hao, Y. Huang, Status and prospects in sulfur-carbon composites as cathode materials for rechargeable lithium−sulfur batteries, Carbon 92 (2015) 41–63.

[6] A. Rosenman, E. Markevich, G. Salitra, D. Aurbach, A. Garsuch, F. Chesneau, Review on Li−Sulfur battery systems: an integral perspective, Adv. Energy Mater. 5 (2015) 150–212.

[7] X. Ji, K. T. Lee, L. Nazar, A highly ordered nanostructured carbon-sulphur cathode for lithium−sulphur batteries, Nat. Mater. 8 (2009) 500–506.

[8] B. Zhang, X. Qin, G. R. Li, X. P. Gao, Enhancement of long stability of sulfur cathode by encapsulating sulfur into micropores of carbon spheres, Energy Environ. Sci. 3 (2010) 1531–1537.

[9] G. He, X. Ji, L. Nazar, High “C” rate Li-S cathodes: sulfur imbibed bimodal porous carbons, Energy Environ. Sci. 4 (2011) 2878–2883.

[10] S. Xin, L. Gu, N. Zhao, Y. Yin, L. Zhou, Y.. Guo, L. Wang, Smaller sulfur molecules promise better lithium−sulfur batteries, J. Am. Chem. Soc. 134 (2012) 18510–18513.

[11] P. Strubel , S. Thieme , T. Biemelt , A. Helmer, M. Oschatz, J. Brückner , H. Althues, S. Kaskel, ZnO hard templating for synthesis of hierarchical porous carbons with tailored porosity and high performance in lithium−sulfur battery, Adv. Funct. Mater. 25 (2015) 2 287–297.

[12] R. Sahore, B. Levin, M. Pan, D. Muller, F. DiSalvo, E. Giannelis, Design principles for optimum performance of porous carbons in lithium−sulfur batteries, Adv. Energy Mater. 6 (2016) 14 1600134–1600143.

[14] Z. Li, Y. Jiang, L. Yuan, Z. Yi, C. Wu, Y. Liu, P. Strasser, Y. Huang, A highly ordered meso@microporous carbon-supported sulfur @smaller sulfur core-shell structured cathode for Li–S batteries, ACS Nano 8 (2014) 9295–9303.

[15] N. Jayaprakash, J. Shen, S. Moganty, A. Corona, L. Archer, Porous hollow

carbon@sulfur composites for high-power lithium−sulfur batteries, Angew. Chem. 123 (2011) 6026–6030.

[16] C. Zhang, H. Wu, C. Yuan, Z. Guo, X. W. Lou, Confining sulfur in double-shelled hollow carbon spheres for lithium–sulfur batteries, Angew. Chem. Int. Ed. 51 (2012) 9592–9595.

[17] G. He, S. Evers, X. Liang, M. Cuisinier, A. Garsuch, L. F. Nazar, Tailoring porosity in carbon nanospheres for lithium−sulfur battery cathodes, ACS Nano 7 (2013) 10920–10930.

[18] W. Li, Z. Z. Lu, H. Yao, Z. Seh, K. Yan, G. Zheng, Y. Cui, A sulfur cathode with pomegranate-like cluster structure, Adv. Energy Mater. 5 (2015) 16 1500211–1500218.

[19] H. Wang, Y. Yang, Y. Liang, J. T. Robinson, Y. Li, A. Jackson, Y. Cui, H. Dai, Graphene-wrapped sulfur particles as a rechargeable lithium−sulfur battery cathode material for high capacity and cycling stability, Nano Lett. 11 (2011) 2644–2647.

[20] J. Huang, X. Liu, Q. Zhang, C. Chen, M. Zhao, S. Zhang, W. Zhu, W. Qian, F. Wei, Entrapment of sulfur in hierarchical porous graphene for lithium−sulfur batteries with high rate performance from -40 to 60 ºC, Nano Energy 2 (2013) 314–321.

[21] G. Zhou, S. Pei, L. Li, D. Wang, S. Wang, K. Huang, L. Yin, F. Li, H. Cheng, A graphene–pure-sulfur sandwich structure for ultrafast long-life lithium−sulfur batteries, Adv. Mater. 26 (2014) 625–631.

[22] L. Sun, D. Wang, Y. Luo, K. Wang, W. Kong, Y. Wu, L. Zhang, K. Jiang, Q. Li, Y. Zhang, J. Wang, S. Fan, Sulfur embedded in a mesoporous carbon nanotube network as a binder-free electrode for high-performance lithium-sulfur batteries, ACS Nano 10 (2016) 1300–1308.

[23] Y. Zhao, W. Wu, J. Li, Z. Xu, L. Guan, Encapsulating MWNTs into hollow porous

carbon nanotubes: a tube-in-tube carbon nanostructure for high-performance lithium−sulfur batteries, Adv. Mater. 26 (2014) 5113–5118.

[24] L. Ji, M. Rao, S. Aloni, L. Wang, E. J. Cairns, Y. Zhang, Porous carbon nanofiber-sulfur composite electrodes for lithium/sulfur cells, Energy Environ. Sci. 4 (2011) 5053–5059.

[25] S. Lu, Y. Cheng, X. Wu, J. Liu, Significantly improved long-cycle stability in high-rate Li-S batteries enabled by coaxial graphene wrapping over sulfur-coated carbon nanofibers, Nano Lett. 13 (2013) 2485–2489.

[26] M. Song, Y. Zhang, E. Cairns, A long-life, high-rate lithium/sulfur cell: a multifaceted approach to enhancing cell performance, Nano Lett. 13 (2013) 5891–5899.

[27] Z. Wang, Y. Dong, H. Li, Z. Zhao, H. Wu, C. Hao, S. Liu, J. Qiu, X. Lou, Enhancing lithium−sulphur battery performance by strongly binding the discharge products on amino-functionalized reduced graphene oxide, Nature Comm. 5 (2014) 5002.

[28] Q. Pang, L. F. Nazar, Long-life and high-areal-capacity Li−S batteries enabled by a light-weight polar host with intrinsic polysulfide adsorption, ACS Nano 10 (2016) 4111–4118.

[29] J. Song, T. Xu, M. Gordin, P. Zhu, D. Lv, Y. Jiang, Y. Chen, Y. Duan, D. Wang, Nitrogen-doped mesoporous carbon promoted chemical adsorption of sulfur and fabrication of high-areal-capacity sulfur cathode with exceptional cycling stability for lithium−sulfur batteries, Adv. Funct. Mater. 24 (2014) 1243–1250.

[30] C. Hart, M. Cuisinier, X. Liang, D. Kundu, A. Garsuch, L. Nazar, Rational design of sulphur host materials for Li−S batteries: correlating lithium polysulphide adsorptivity and self-discharge capacity loss, Chem. Commun. 51 (2015) 2308–2311.

[31] X. Liang, C. Kwok, F. Marzano, Q. Pang, M. Cuisinier, H. Huang, C. J. Hart, D. Houtarde, K. Kaup, H. Sommer, T. Brezesinski, J. Janek, L. Nazar, Tuning transition metal oxide-sulfur interactions for long life lithium sulfur batteries: the “Goldilocks” principle, Adv. Eng. Mater. 6 (2016) 1501636.

[32] J. Zheng, J. Tian, D. Wu, M. Gu, W. Xu, C. Wang, F. Gao, M. Engelhard, J. Zhang, J. Liu, J. Xiao, Lewis acid-base interactions between polysulfides and metal organic framework in lithium sulfur batteries, Nano Lett. 14 (2014) 2345–2352.

[33] Y. Su, A. Manthiram, Lithium−sulphur batteries with a microporous carbon paper as a bifunctional interlayer, Nature Commun. 3 (2012) 1166.

[34] Q. Tang, Z. Shan, L. Wang, X. Qin, K. Zhu, J. Tian, X. Liu, Nafion coated sulfur-carbon electrode for high performance lithium−sulfur batteries, J. Power Sources 246 (2014) 253–259.

[35] H. Yao, K. Yan, W. Li, G. Zheng, D. Kong, Z. W. Seh, V. Narasimhan, Z. Liang, Y. Cui, Pie-like electrode design for high-energy density lithium−sulfur batteries, Energy Environ. Sci.7 (2014) 3381–3390.

[36] S. Chung, A. Manthiram, A polyethylene glycol-supported microporous carbon coating as a polysulfide trap for utilizing pure sulfur cathodes in lithium−sulfur batteries, Adv. Mater. 26 (2014) 7352–7357.

[37] K. Park, J. H. Cho, J.-H. Jang, B.-C. Yu, A. T. De La Hoz, K. M. Miller, C. J. Ellison, J. B. Goodenough, Trapping lithium polysulfides of a Li−S battery by forming lithium bonds in a polymer matrix, Energy Environ. Sci. 8 (2015) 2389–2395.

[38] J. Hwang, H. Kim, S. Lee, J. Lee, A. Abouimrane, M. Khaleel, I. Belharouak, A.

Manthiram, Y. Sun, High-energy, high-rate, lithium−sulfur batteries: synergetic effect of hollow TiO_2-webbed carbon nanotubes and a dual functional carbon-paper interlayer, Adv. Energy Mater. 6 (2016) 150 1501480–1501487.

[39] M. Wu, X. Xiao, N. Vukmirovic, S. Xun, P. K. Das, X. Song, P. Olalde-Velasco, D. Wang, A. Weber, L. Wang, V. Battaglia, W. Yang, G. Liu, Toward an ideal polymer binder design for high-capacity battery anodes, J. Am. Chem. Soc. 135 (2013) 32 12048–12056.

[40] Z. Seh, Q. Zhang, W. Li, G. Zheng, H. Yao, Y Cui. Stable cycling of lithium sulfide cathodes through strong affinity with a bifunctional binder, Chem. Sci. 4 (2013) 3673–3677.

[41] M. Lacey, F. Jeschull, K. Edström, D. Brandell, Functional, water-soluble binders for improved capacity and stability of lithium−sulfur batteries. J. Power Sources 264 (2014) 8–14.

[42] G. Li, W. Cai, B. Liu, Z. Li, A Multi-functional binder with lithium ion conductive polymer and polysulfide absorbents to improve cycleability of lithium−sulfur batteries, J. Power Sources 294 (2015) 187–192.

[43] G. Ai, Y. Dai, Y. Ye, W. Mao, Z. Wang, H. Zhao, Y. Chen, J. Zhu, Y. Fu, V. Battaglia, J. Guo, V. Srinivasan, G. Liu, Investigation of surface effects through the application of the functional binders in lithium sulfur batteries, Nano Energy 16 (2015) 28–37.

[44] J. Wang, Z. Yao, C. Monroe, J. Yang, Y. Nuli, Carbonyl-β-cyclodextrin as a novel binder for sulfur composite cathodes in rechargeable lithium batteries, Adv. Funct. Mater. 23 (2013) 1194–1201.

[45] F. Zeng, W. Wang, A. Wang, K. Yuan, Z. Jin, Y. Yang, Multidimensional polycation β−cyclodextrin polymer as an effective aqueous binder for high sulfur loading cathode in

lithium−sulfur batteries, ACS Appl. Mater. Interfaces 7 (2015) 47, 26257–26265.

[46] G. Li, M. Ling, Y. Ye, Z. Li, J. Guo, Y. Yao, J. Zhu, Z. Lin, S. Zhang, Acacia Senegal-inspired bifunctional binder for longevity of lithium−sulfur batteries, Adv. Energy Mater. 5 (2015) 1500878.

[47] P. Bhattachary, M. Nandasiri, D. Lv, A. Schwarz, J. Darsell, W. Henderson, D. Tomalia, J. Liu, J. Zhang, J. Xiao, Polyamidoamine dendrimer-based binders for high-loading lithium−sulfur battery cathodes, Nano Energy 19 (2016) 176–186.

[48] W. Chen, T. Qian, J. Xiong, N. Xu, X. Liu, J. Liu, J. Zhou, X. Shen, T. Yang, Y. Chen, C. Yan, A new type of multifunctional polar binder: toward practical application of high energy lithium sulfur batteries, Adv. Mater. 29 (2017) 1605160.

[49] S. S. Zhang, New insight into liquid electrolyte of rechargeable lithium/sulfur battery, Electrochim. Acta 97 (2013) 226–230.

[50] S. Zhang, Binder based on polyelectrolyte for high capacity density lithium/sulfur battery, J. Electrochem. Soc. 159 (2012) 8 1226–1229.

[51] P. Xiang, Z. Ye, Hyperbranched polyethylene ionomers containing cationic tetralkylammonium ions synthesized by Pd−diimine-catalyzed direct ethylene copolymerization with ionic liquid comonomers, Macromolecules 48 (2015) 6096−6107.

[52] S. Zhang, N. Sun, X. He, X. Lu, X. Zhang, Physical properties of ionic liquids: database and evaluation, J. Phys. Chem. Ref. Data, 35 (2006) 4 1475–1517.

[53] X. Liang, C. Hart, Q. Pang, A. Garsuch, T. Weiss, L. F. Nazar, A highly efficient polysulfide mediator for lithium–sulfur batteries, Nat. Commun. 6 (2015) 5682.

[54] I. J. Kartio, C. I. Basilio, R. H., Yoon, An XPS study of sphalerite activation by copper,

Langmuir 14 (1998) 5274–5278.

[55] R. Ponraj, A. G. Kannan, J. H. Ahn, D. W. Kim, Improvement of cycling performance of lithium−sulfur batteries by using magnesium oxide as a functional additive for trapping lithium polysulfide, ACS Appl. Mater. Interfaces 8 (2016) 4000−4006.

[56] S. Evers, T. Yim, L. F. Nazar, Understanding the nature of absorption/adsorption in nanoporous polysulfide sorbents for the Li−S battery, J. Phys. Chem. C 116 (2012) 19653−19658.

[57] Q. Wang, N. Yan, M. Wang, C. Qu, X. Yang, H. Zhang, X. Li, H. Zhang, Layer-by-layer assembled C/S cathode with trace binder for Li−S battery application, ACS Appl. Mater. Interfaces 7 (2015) 25002−25006.

[58] M. Lacey, F. Jeschull, K. Edström, D. Brandell, Why PEO as a binder or polymer coating increases capacity in the Li-S system, Chem. Commun. 49 (2013) 8531–8533.

[59] G. Xu, Q. Yan, A. Kushima, X. Zhang, J. Pan, J. Li, Conductive graphene oxide-polyacrylic acid (GOPAA) binder for lithium-sulfur battery, Nano Energy 31 (2017) 568−574.

[60] X. Hong, J. Jin, Z. Wen, S. Zhang, Q. Wang, C. Shen, K. Rui, On the dispersion of lithium-sulfur battery cathode materials effected by electrostatic and stereo-chemical factors of binders, J. Power Sources 324 (2016) 455–461.

[61] L. Yuan, X. Qiu, L. Chen, W. Zhu, New insight into the discharge process of sulfur cathode by electrochemical impedance spectroscopy, J. Power Sources 189 (2009) 127–132.

[62] Z. Guo, B Zhang, D. Lia, T. Zhao, P. Coxon, C. Harris, R. Hao, Y. Liu, K. Xi, X. Li, A mixed microporous-low-range mesoporous composite with high sulfur loading from

hierarchically-structured carbon for lithium sulfur batteries, Electrochim. Acta 230 (2017) 181–188.

Figure Captions

Figure 1. (a) Schematic representation of PVDF and PDADMA-X binders with different counter ions, and (b) the possible interactions between the PDADMA-X and polysulfides in the sulfur cathodes.

Figure. 2. Photograph (a, b) and UV spectra (c, d) of Li_2S_4-contained DOL-DME mixed solutions at different mass ratios: without absorbent (blank) and with absorbents of PVDF, PDADMA-Cl, PDADMA-T, PDADMA-B and PDADMA-P, respectively.

Figure 3. XPS study on the interaction between lithium polysulfide and PDADMA-T: (a)–(c) S_{2p} spectra, (d)–(f) Li_{1s} spectra, (g)–(i) N_{1s} spectra of pure Li_2S_4, PDADMA-T containing adsorbed Li_2S_4, and pure PDADMA-T, respectively.

Figure 4. Image of (a) the surface of electrodes (sulfur loading, 1.0 mg cm^{-2}) and (b) the electrolyte solutions soaking the electrodes fabricated with different polymer binder for 2 weeks.

Figure 5. (a)–(e) CV curves of cathodes fabricated with the different polymer binders during the first 10 cycles; (f) comparison of their 10^{th} cycle CV curves. Scan rate: 0.1 mV s^{-1}.

Figure 6. Rate performances of cathodes fabricated with the various polymer binders. Cut-off

voltage: 1.5–3.0 *vs*. Li^+/Li anode; sulfur loading density: 1.0 mg cm^{-2}.

Figure 7. Galvanostatic cycling performance of the various cathodes with different binders within 1.5–3.0 V (*vs*. Li^+/Li): (a) discharge capacity and Columbic efficiency curves at 0.2 C; (b) charge-discharge voltage profiles at the 50^{th} cycle at 0.2C; (c) discharge capacity and Columbic efficiency curves at 0.5 C.

Figure 8. Cycling performance of cathodes fabricated with PVDF and PDADMA-T, respectively, at a sulfur loading density of 3.0 mg cm^{-2} within 1.7–2.8 V (*vs*. Li^+/Li) at 0.2C.

Figure 9. Nyquist plots of the various cathodes (a) before cycling and (b) after 16 cycles within 1.7–2.8 V at 0.2C.

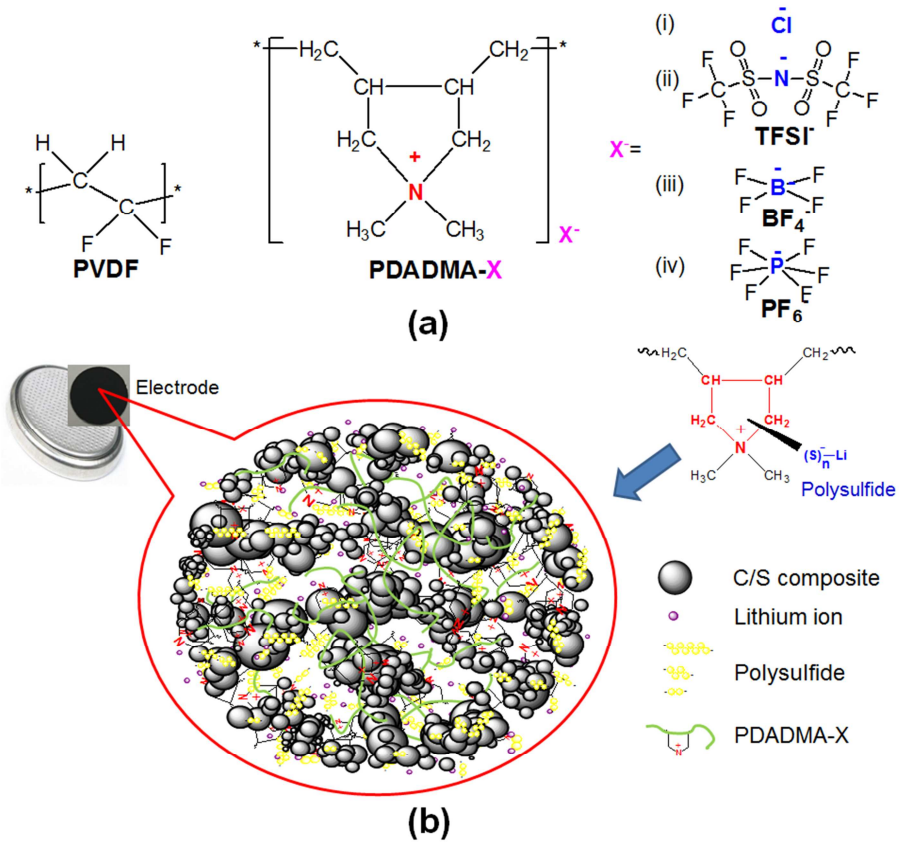

(Figure 1)

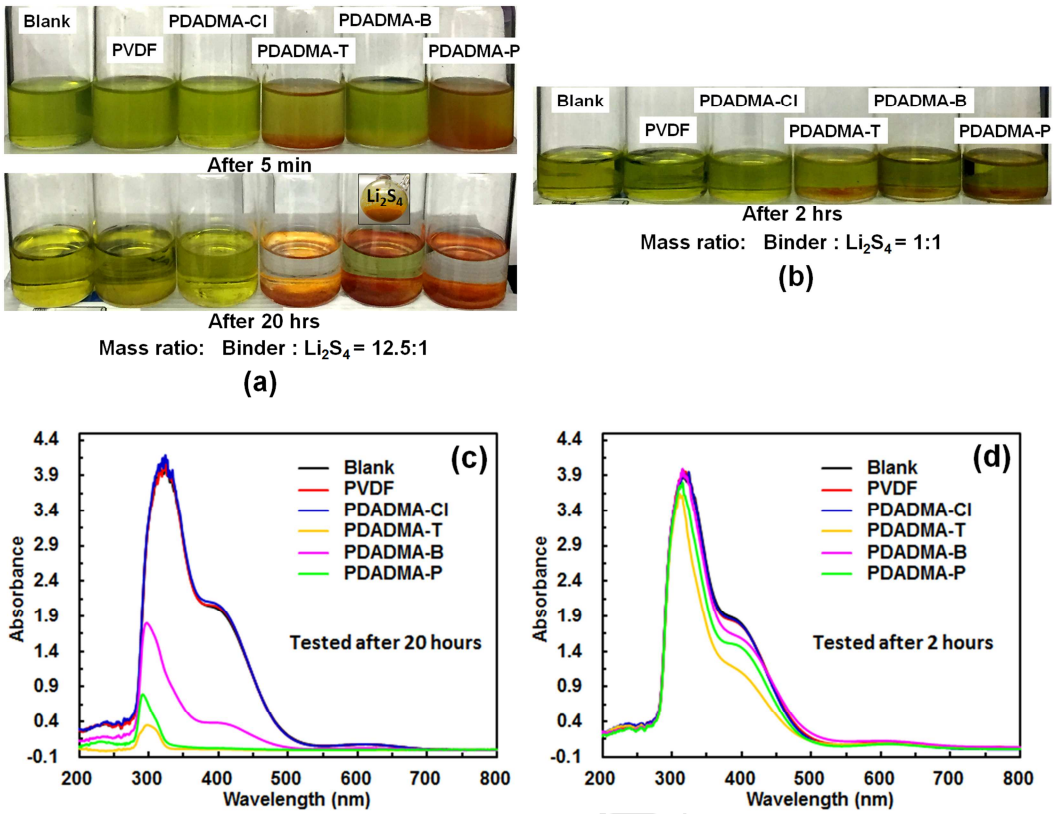

(Figure 2)

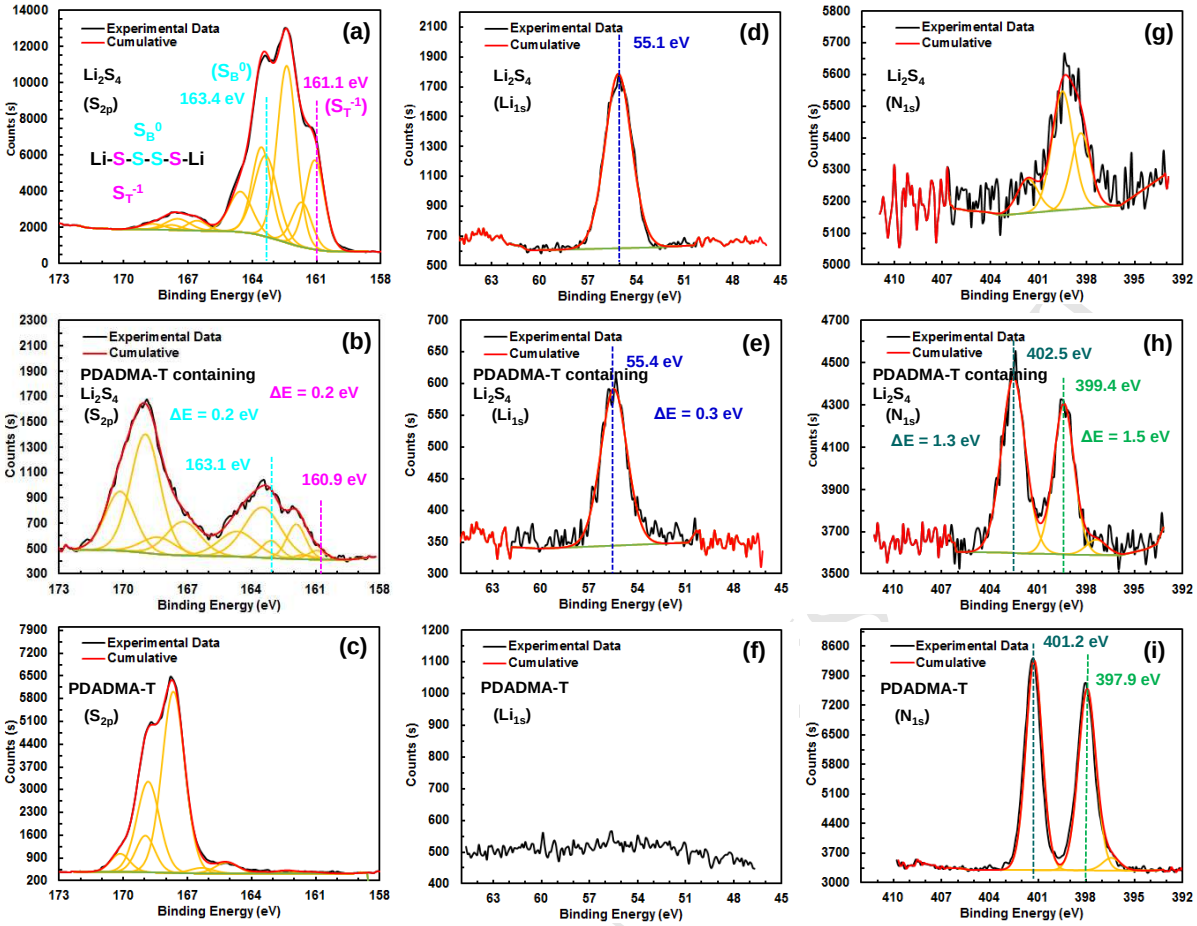

(Figure 3)

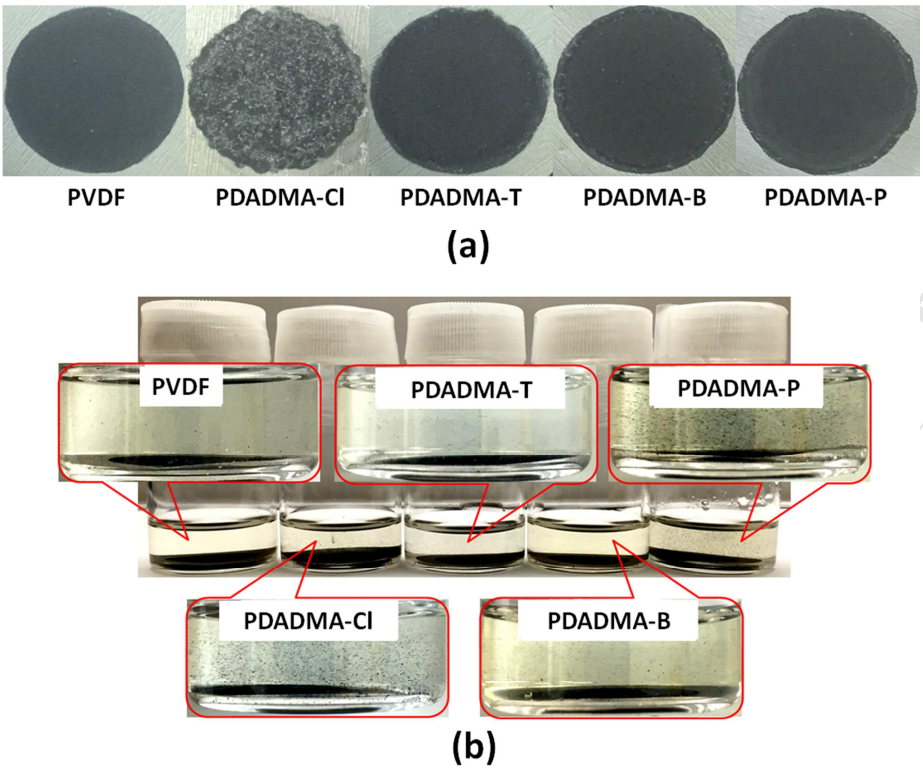

(Figure 4)

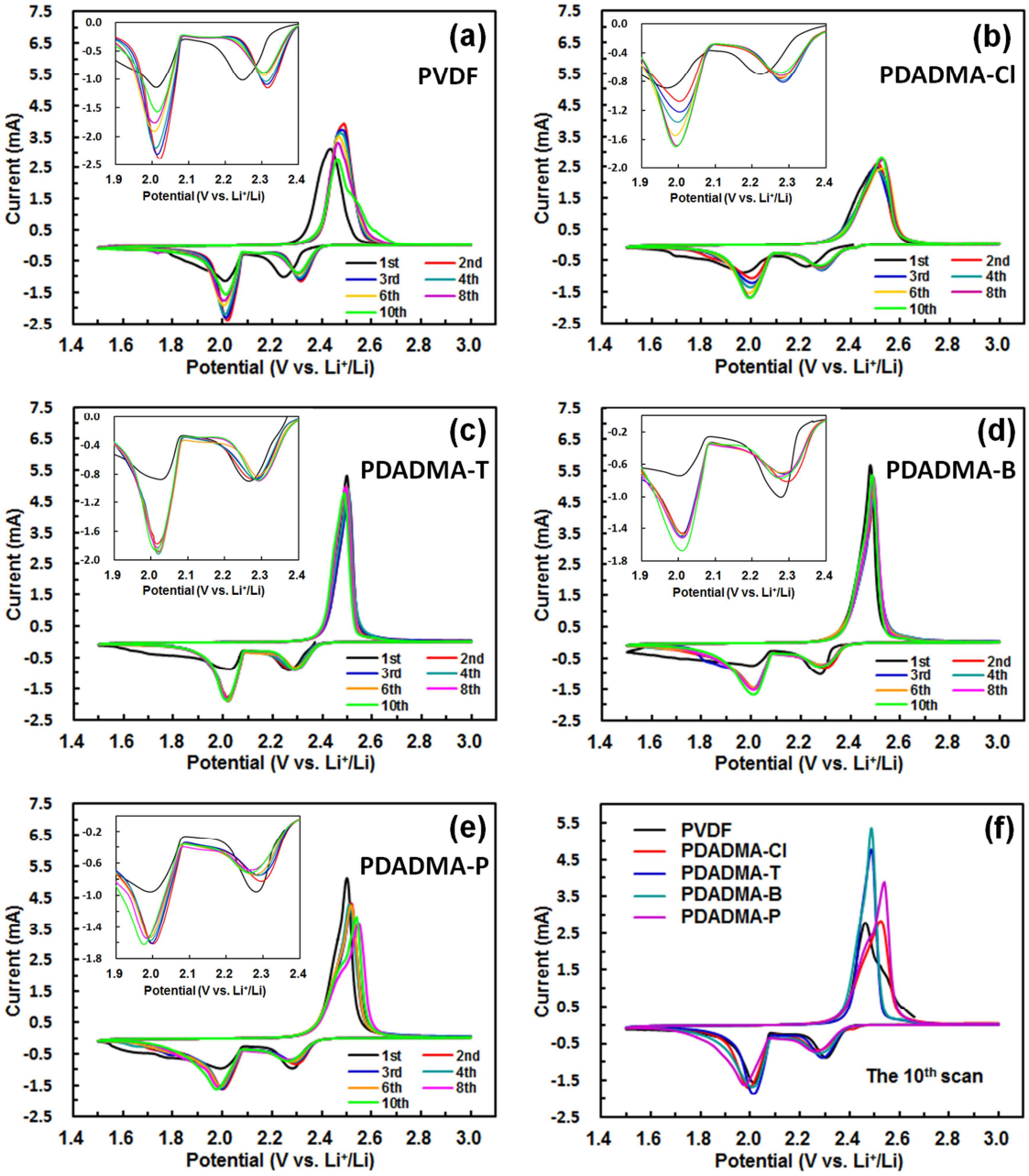
(a)
PVDF
(b)
PDADMA-Cl
(c)
PDADMA-T
(d)
PDADMA-B
(e)
PDADMA-P
(f)
PVDF
PDADMA-Cl
PDADMA-T
PDADMA-B
PDADMA-P
The 10th scan
1st
2nd
3rd
4th
6th
8th
10th
Current (mA)
Potential (V vs. Li+/Li)

(Figure 5)

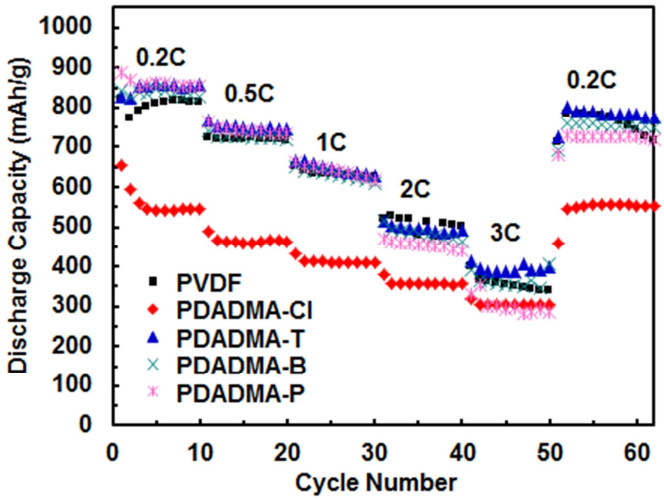

(Figure 6)

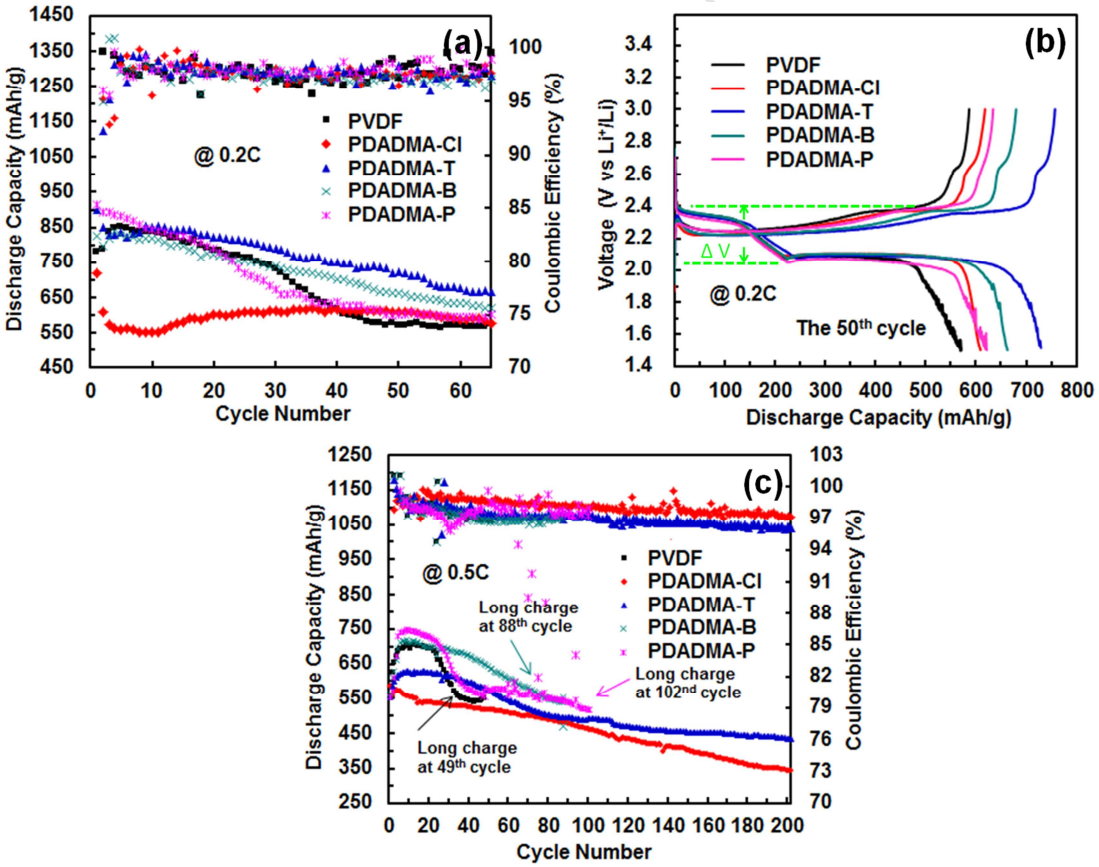

(Figure 7)

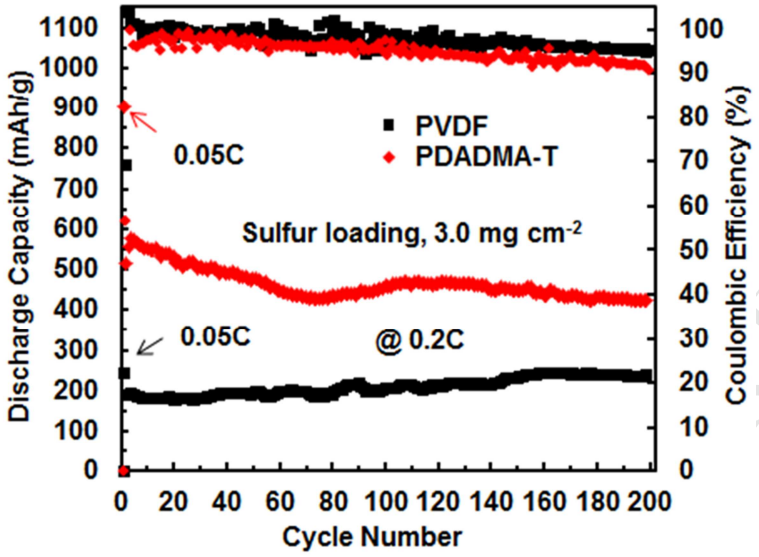

(Figure 8)

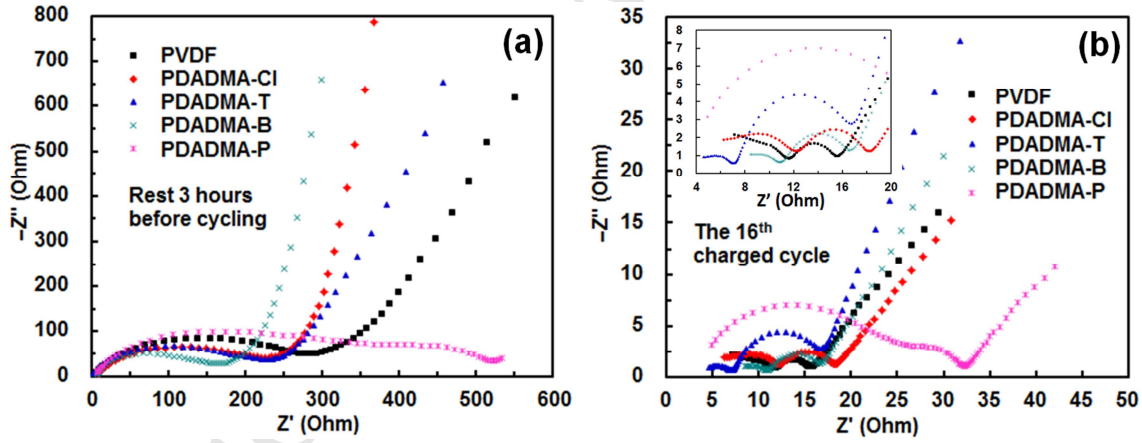

(Figure 9)